Korean Journal of Remote Sensing, Vol.19, No.5, 2003, pp.403~409

A Defective Detector Suppression in the Short Wave Infrared Band of SPOT/VEGETATION-1

Kyung-Soo Han* and Young-Seup Kim**

CNRM / GMME / MATIS, Meteo-France, France*

Dept. of Satellite Information Science, Pukyong National University**

Abstract : Since SPOT4 satellite contained VEGETATION 1 sensor launched, the noise in VEGETATION data was occasionally arisen a difficulty for the data traitement. Blind line noise types were studied in VEGETATION-1 short wave infrared channel(SWIR). In order to provide a precis product, the procedure for removing this noise is strongly recommended. In the case that the blind values are clearly distinguished from contamination-free values a simple threshold method was applied, while a changeable threshold method was used for the blind value mixed with contamination-free values. New algorithm presented in this study is consists of two method for each type of SWIR blind. After removing blind line, there were again some residual pixels of blind, because the threshold is not determinated sufficiently low. Lower threshold could remove the blind line as well as the contamination-free pixels. Nevertheless, the results showed a good qualitative improvement as compared with other algorithm.

Key Words : SPOT4, VEGETATION Sensor, SWIR Blind, Suppression.

1. Introduction

All satellite measurements contain noise. Image noise is any unwanted signal or disturbance in an image. If the noise is severe enough to degrade the quality of the image, *i.e.*, to impair extraction of information from the image, an attempt for the noise suppression is warranted. In digital images processing, therefore, the extraction of noise is an important operation to accurately transform into second level remote sensing products. Since SPOT4 satellite contained VEGETATION 1 sensor launched, the noise in VEGETATION data was occasionally arisen a difficulty for the data traitement. In the viewing instruments, especially in the Short Wave Infrared (SWIR), some of 300 detectors in the SWIR camera are blind because located between two detector chips, and some others are declared defective consequently to proton shocks (Passot, 2000). So called SWIR blind or defective SWIR detector signifies that some oblique lines with high values are often visible in the SWIR band. In the original raw image, the blind line is appeared vertically. In this case, we can easily detect, but VEGETATION programme do not actually provide the original raw image. Because whole products (P, S, and D) of VEGETATION data are porvided after pre-processing for the geometric correction, the blind line in VEGETATION SWIR channel, therefore, appears obliquely. This brings

Received 20 March 2003; Accepted 20 August 2003.

on a difficulty to easily detect this blind.

Various methods were presented to noise removal in the three last decades: Tukey median filter (Frieden, 1976; Wecksung and Campbell, 1974); linear noise filter (Schowengerdt, 1983); non-linear noise filter (Chavez and Soderblum, 1975); infinite impulse response filter (Ziou, 1991); noise cheating (Zweig *et al.*, 1976). In some cases, sensor calibration data and even test images may exist that are sufficiently comprehensive to estimate noise parameters. Unfortunately, however, these types of data are often incomplete or the noise is unexpected (Schowengerdt, 1983). In the case of VEGETATION 1, the noise suppression is not easy process using the methods that we presented above. Fillol (2001) suggested a threshold method to remove the blind for SWIR reflectance value. Mayaux *et al.* (2001) used an indirect removing algorithm using 10-day minimum value compositing technique.

However, Fillol's method did not produce a suitable result for our test images, because it assumed that the blinds would be characterized as homogeneity in the SWIR band. Therefore, the threshold of this method was adopted for a part of SWIR blinds. The minimum value compositing algorithm of Mayaux *et al.*(2001) permits to remove the almost blind effect through average of minimum values during specific time series, but it has a limit that cannot directly detect SWIR blind in original image.

In this study, we will consider and discuss on the types of SWIR blind of VEGETATION1 and present a new algorithm to detect it.

2. Characteristic on the Blinds of VEGETATION 1 SWRI Channel

Fig. 1 shows an image composed by a procedure of the Bidirectional Reflectance Distribution Function (BRDF) correction for a period from 240 to 270 Julian day (31days), 2000, with three channels (visible(b2), near-infrared (b3) and SWIR) of VEGETATION 1 over the frontier area of France, Belgium, Switzerland and Germany. Although the feature of blind became slightly weak (not shown here) by 31-day composite, about 20 blinds were digitally and visibly detected. In remote sensing for surface interpretation and environmental monitoring researches, image compositing or/and BRDF correction using integration of time series images are essential process. In particular, if the numbers of scenes involving the SWIR band blind are existed during

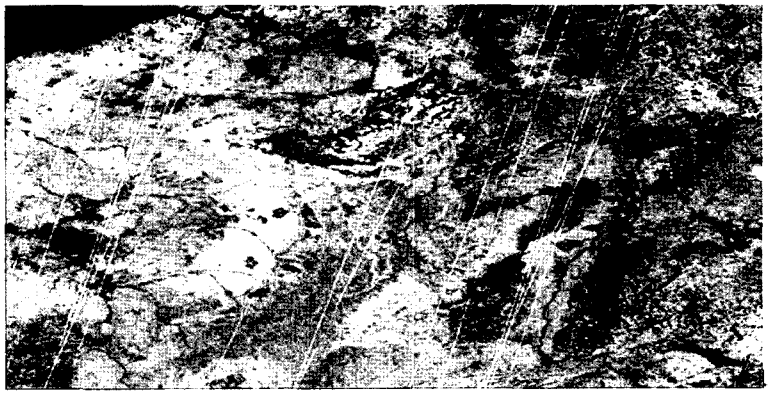

Fig. 1. Composite image without SWIR blind suppression processing for a period from 240 to 270 Julian day 2000, with three channels(visible(b2), near-infrared(b3) and SWIR).

composite period as shown in Fig. 1, the quality of composite image is dramatically decreased.

In this study we found two major types of SWIR blind according to distribution shape of pixel values constituting a blind line. These types are displayed in Fig. 2 (Julian day 267, 2000) and 3 (Julian day 255, 2000), and can be describe as follows;

Type 1 (Fig. 2):

- The blind consists of core layer and dilatation layer.
- The reflectance values in core layer are sufficiently high in comparison with the values of other targets.
- Dilatation layer is formed by lower values than neighbor pixel values.

Type 2 (Fig. 3):

- The boundary between a blind line and the contamination-free pixel zone is indistinct.
- It is difficult to find the layer as a dilatation of Type 1.

Therefore it indicates that the blind removing for these two types is impossible using an identical method, such as single threshold method(Fillol, 2000). This paper presents two different methods to detect for the types described above.

3. Suppression Processing

1) Method 1

Type 1 represents a typical case of SWIR blind. The analysis was performed in a row unit to suppress this isolated noise. As described above, the core layer of Type 1 are sufficiently high in comparison with the other pixel values in a row. Therefore, we can apply a threshold method for the

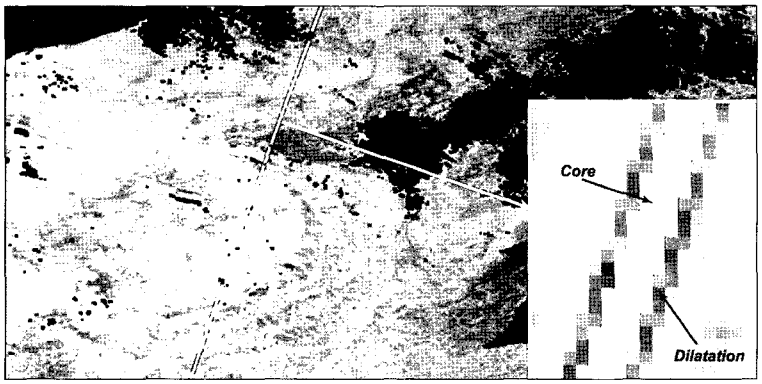

Fig. 2. Example image of SWIR blind(267 Julian day, 2000).

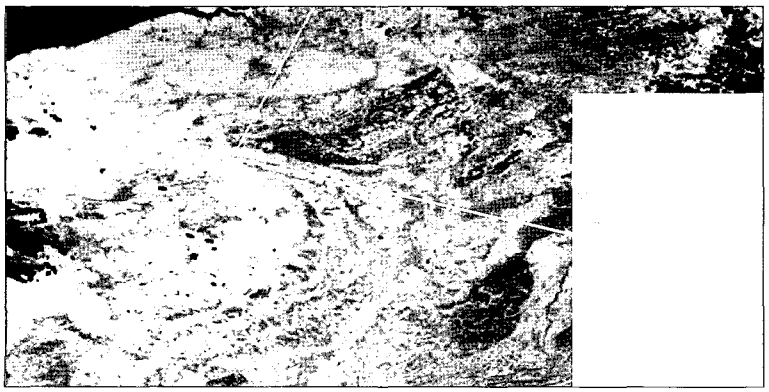

Fig. 3. Example image of SWIR blind(255 Julian day, 2000).

core value in this case. The threshold value was absolutely determined by results of relative comparisons for contamination-free values in each row in an image. Fig. 4 shows three examples of column profiles for pixel values in a row (lows 71, 175 and 388) for image shown in Fig. 2. These profiles indicate three channel reflectance values after cloud mask. We named the picked values in SWIR channel(marked with gray oval in Fig. 4) to the blind core layer. SWIR channel, according to VEGETATION user guide (<http://www.spotimage.fr/ data/images/vege/VEGETAT/book_1/e_frame.htm>), has a surface reflectance range from 0 to 0.6 allowing for saturation for some land covers, as snow or bright soils, and for clouds.

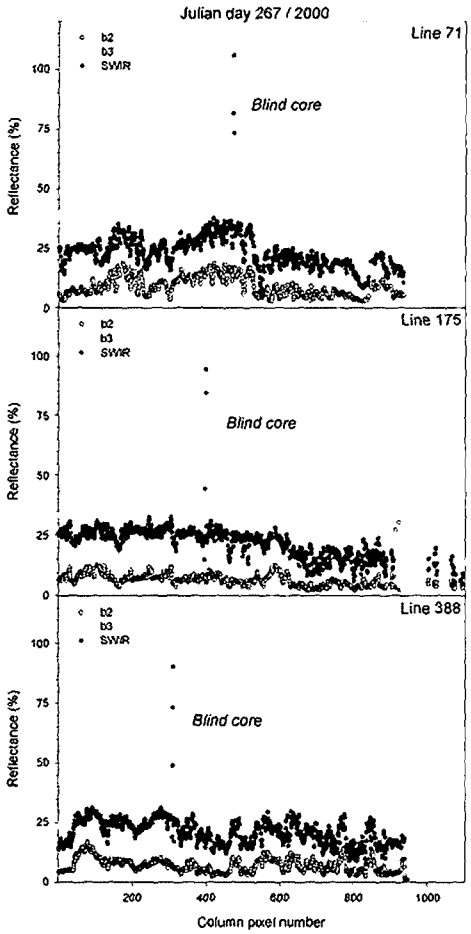

Fig. 4. Column profiles of three sample rows for channel reflectances in image(267 Julian day, 2000).

Fillol (2001) determined the blind when SWIR reflectance is above 0.75. However, this threshold could not completely detect not only blind core layer but also dilatation layer in our study. We found that the values of blind core layer are distributed to a range above 0.45 (Fig. 4).

As shown in Fig. 2, the dilatation layer is consisted of by lower values than neighbor pixel values. In spite of this feature, it is very difficult to digitally isolate it from contamination-free pixel values, because its values are not sufficiently or recognizably low as compared with the others (*i.e.*, it is lower than neighbor pixel values, but it is mixed with all contamination-free values in a row). The dilation layer is formed at two boundaries between the core layer and contamination-free pixel zone by one pixel range (Fig. 2). By this regulation, the dilation layer can be detected and expressed as follows;

$$D_s = P_s(i-1, j) \quad (1)$$

$$D_e = P_e(i+1, j) \quad (2)$$

where D_s and D_e are dilatation values of both side, P_s (i, j) is a pixel started a core layer, and $P_e(i, j)$ is a pixel ended a core layer. Fig. 5 shows an excellent example of result (case (b)) for Type 1 after our suppression algorithm.

2) Method 2

Unlike Type1, it is indistinct to visibly distinguish the blind values from the contamination-free pixel zone as

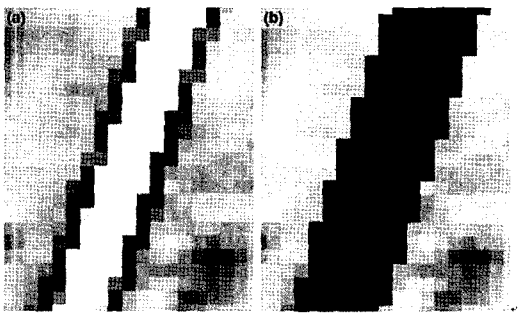

Fig. 5. Zooming images of before (a) and after (b) SWIR suppression using simple threshold method.

shown in Fig. 3. The column profiles in Fig. 6 clearly show a limitation to apply a threshold method to this type (the arrows indicate the locations of blind values). Similar to dilatation layer of Type 1, these values are lower than neighbor pixel values, but it is mixed with all contamination-free values in a row. In addition, it is not easy to find any regulation or recognizable feature. Therefore, a method has been suggested in this study through a coupling with other channel data.

In VEGETATION sensor, there are some pixels having same reflectance values in b3 and SWIR channels, while b2 and SWIR channels preserve a gap between their reflectance values (Fig. 6). It means that the difference of b2 and SWIR channel reflectances can be a useful tool to detect an abnormal value of SWIR channel. We analyzed with its square value to amplify this difference.

Fig. 7 depicts column profiles of $(SWIR-b2)^2$ values for same condition with Fig. 6, and a good indicator of SWIR blind values. Nevertheless, it is also difficult to decide a threshold by $(SWIR-b2)^2$ value. For example, if a threshold is decided to 370 by top of Fig. 7, it can be dangerous for other rows such as row 175 (middle of Fig. 7). The changeable threshold value has been used by its standard deviation value of each row. That is,

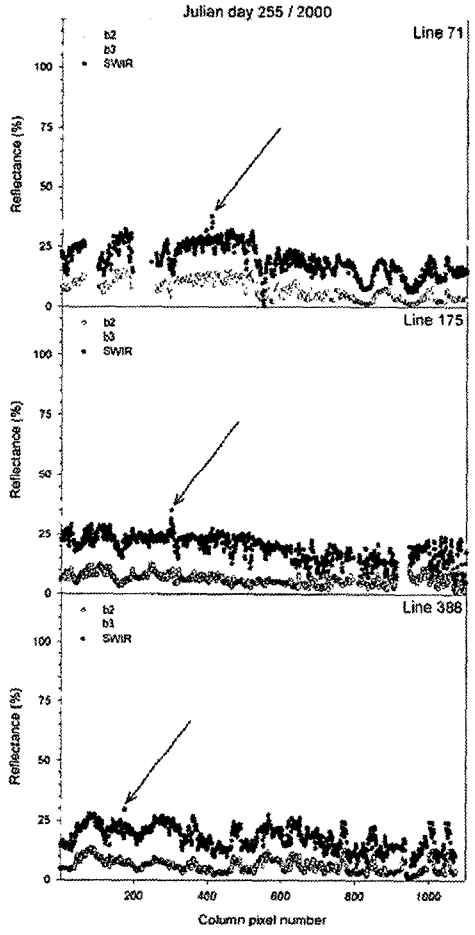

Fig. 6. Column profiles of three sample rows for channel reflectances in image (255 Julian day, 2000).

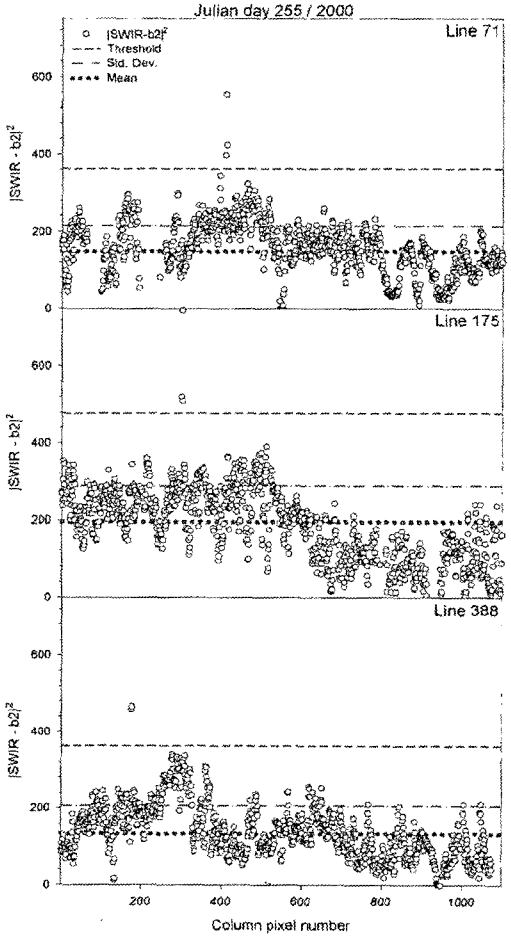

Fig. 7. Column profiles of three sample rows for (b2-SWIR)2 values in image (255 Julian day, 2000).

$$Threshold = \overline{\nabla} + 3 \cdot \sigma_{\nabla} \quad (3)$$

where $\overline{\nabla}$ is the mean value of $\nabla = (\text{SWIR-b2})^2$ values in a row, and σ_{∇} is the standard deviation value of ∇ values in a row. The threshold values of each row are indicated with short dashed line in Fig. 7. A non-detected blind line by method of Fillol(2001) and Type 1 were well suppression by a changeable threshold scheme of Eq. (3) (Fig. 8).

Fig. 9 shows an image composed after suppression SWIR blinds using the present method. In comparison with Fig. 1, the blind effect during composite period (240~270 Julian days, 2000) was clearly removed.

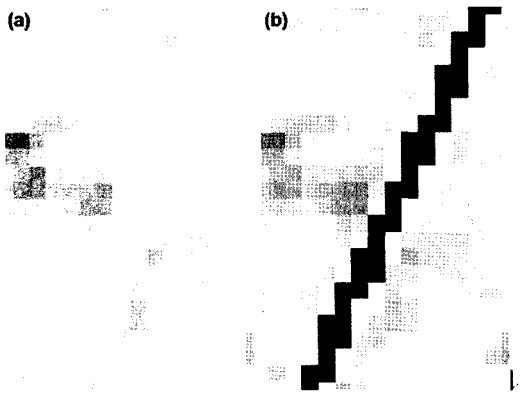

Fig. 8. Zooming images of before (a) and after (b) SWIR suppression using changeable threshold method.

4. Summary

For correctly processed imagery in SPOT-VEGETATION sensor, we carried out a blind suppression work in SWIR channel with newly presented scheme in this study. Two different methods were suggested for two classified types respectively. In the case that the blind values are clearly distinguished from contamination-free values by applying a simple threshold method was applied, while a changeable threshold method was used for the blind value mixed with contamination-free values. The result showed a good qualitative and quantitative improvement as compared with other algorithm. However, in the case that the blind values are mixed with contamination-free values, we did not obtain a perfect suppression results. After removing blind line, there were again some residual pixels of blind, because the threshold is not determinated sufficiently low. Lower threshold could remove the blind line as well as the contamination-free pixels. The pattern classification, such as, the clustering, the artificial neural network, or supervised classification, may help to provide more precise product.

Fig. 9. Image composed after SWIR blind suppression processing for a period between 240 and 270 Julian day 2000 (31days), and three channels (visible (b2), near-infrared(b3) and SWIR).

Acknowledgement

SPOT-VEGETATION daily synthesis data was produced by CNES (Centre National d tudes Spatiales).

References

Chavez, P. S. and L. A. Soderblum, 1975. Simple high-speed digital image processing to remove quasi-coherent noise patterns, Proc. Am. Soc. Photogrammetry, pp. 595-600.

Fillol, E., P. Kennedy, and S. Folving, 2001. Test of forest classification over Bavaria (Germany) using a SPOT-VGT pixel mosaic, *Proc. Method GLC 2000 Workshop*, Ispra, Italy, CD-Rom.

Frieden, B. R., 1976. A new restoring algorithm for preferential enhancement of edge gradients, *J. Opt. Soc. Am.* 66(3): 280-283.

Mayaux, P., V. Gond, and E. Bartholom, 2001. Potential of SPOT 4-VEGETATION data for mapping the forest cover of Madagascar and upper Guinea. *Proc. Method GLC 2000 Workshop*, Ispra, Italy, CD-Rom.

Passot, X., 2000. VEGETATION image processing methods in the CTIV, *Proc. VEGETATION 2000 Conference*, Belgirate, Italy, CD-Rom.

Schowengerdt, R. A., 1983. *Techniques for image processing and classification in remote sensing*. London, Academic Press, 249p.

Wecksung, G. W. and K. Campbell, 1974. Digital image processing at EG&G, *Computer*, 7(5): 63-71.

Ziou, D., 1991. Line detection using an optimal IR filter, *Pattern Recognition*, 24(6): 465-478.

Zweig, H., A. Silverstri, P. Hu, and E. Barrett, 1976. Experiments in digital restoration of defocused grainy photographs by noise cheating and fourier techniques, *Proc. Soc. Photo-optical Instrumentation Engineers*, 74: 10-16.